Journal of Applied Physics

Acoustic coherent perfect absorber and laser modes via the non-Hermitian dopant in the zero index metamaterials

Cite as: J. Appl. Phys. **129**, 234901 (2021); https://doi.org/10.1063/5.0040201
Submitted: 11 December 2020 • Accepted: 03 June 2021 • Published Online: 17 June 2021

Zhongming Gu, Tuo Liu, He Gao, et al.

Journal of Applied Physics ARTICLE scitation.org/journal/jap

Acoustic coherent perfect absorber and laser modes via the non-Hermitian dopant in the zero index metamaterials

Cite as: J. Appl. Phys. **129**, 234901 (2021); doi: 10.1063/5.0040201
Submitted: 11 December 2020 · Accepted: 3 June 2021 ·
Published Online: 17 June 2021

Zhongming Gu,[1,2] Tuo Liu,[1,2] He Gao,[1,2] Shanjun Liang,[3] Shuowei An,[1] and Jie Zhu[1,2,a)]

AFFILIATIONS

[1]The Hong Kong Polytechnic University Shenzhen Research Institute, Shenzhen 518057, People's Republic of China
[2] Research Center for Fluid-Structure Interactions, Department of Mechanical Engineering, The Hong Kong Polytechnic University, Hung Hom, Kowloon, Hong Kong SAR, People's Republic of China
[3]Division of Science, Engineering and Health Studies, College of Professional and Continuing Education, Hong Kong Polytechnic University, Hong Kong SAR, People's Republic of China

Note: This paper is part of the Special Topic on Acoustic Metamaterials 2021.
[a)]**Author to whom correspondence should be addressed:** jiezhu@polyu.edu.hk

ABSTRACT

In this work, we propose a simple scheme to realize an acoustic coherent perfect absorber (CPA) and laser modes by embedding a non-Hermitian dopant in a zero index metamaterial. When the dopant is filled with a loss medium at a specific level, the sample can absorb the incident waves completely. On the other hand, when the dopant is filled with a gain medium, the sample can act as a laser oscillator to boost the incident waves. The theoretical derivation based on the scattering matrix and the numerical simulation based on the finite element method are performed and both show good agreement with each other. We also discover that the CPA and laser modes are very sensitive and can be controlled by adjusting the structure parameters or the relative phase of the incident waves. Moreover, the case that asymmetric incidences have different beam widths is considered. We envision that our work may have potential applications in designing acoustic devices, such as absorbers, transducers, and receivers.

I. INTRODUCTION

Zero index metamaterials (ZIMs) are a kind of artificial structure that can preserve a near-zero refractive index, which has attracted ongoing research interest in different wave systems, such as optics,[1–3] acoustics,[4–7] and elastic waves.[8,9] With their intriguing properties that include an effective extremely large phase velocity, ZIMs can be utilized to realize many extraordinary wave phenomena, such as the tunneling effect,[10] asymmetric transmission,[11,12] and cloaking.[13] Very recently, Liberal *et al.* have proposed the concept of photonic doping by transplanting similar ideas from the field of semiconductor physics.[14,15] The effective parameters, as well as the transmission properties of doped ZIMs, can be modulated as designed. After that, Coppolaro *et al.* extended this work to the non-Hermitian domain.[16] With the tailored distribution of gain and loss in either the dopant or ZIMs, their model enables modulation on the effective parameters in the complex plane and can give rise to unconventional scattering responses. These pioneering works show a feasible approach to wave manipulation with the versatile platform of doped ZIMs.

Coherent perfect absorber (CPA), also known as anti-laser, is considered as the time-reversed counterpart of the optical laser at the threshold.[17–25] With the well-tuned amplitudes and phases of the two incident waves, the outgoing waves will vanish, and the resultant interference in the absorber may lead to a perfect absorption. Contrarily, the mode in which the outgoing wave is extremely enhanced by pumping the incident waves can be regarded as a laser mode. Many efforts have been devoted to studying these intriguing scattering modes based on ZIMs. Luo *et al.* experimentally observed perfect absorption with a solely dissipative dopant embedded in ZIMs.[26] Bai *et al.* simultaneously realized the CPA mode and laser mode by using ZIMs, while devising the complex

design with balanced gain and loss.[27] Thus, the uncomplicated scheme to achieve the CPA and laser modes with a non-Hermitian dopant in ZIMs still deserves a thoughtful study.

Here, we present an ideal model to obtain the CPA and laser modes with a circular dopant implanted in a ZIM. The sample is clamped in the straight waveguide with two ports, which are illuminated by the incident waves with equal amplitude and phase. With the non-Hermitian modulation on the dopant changing from the loss region to the gain region, the CPA mode and laser mode of the system can be stimulated, respectively. Within the CPA mode, the incident energy is absorbed perfectly and the scattering field keeps null. In contrast, within the laser mode, the outgoing wave is extremely magnified compared with the incident wave and radiates to both sides of the waveguide symmetrically. Except the non-Hermitian modulation, both the absorption coefficient and the magnification coefficient are sensitive to the radius of the dopant and the relative phase between the two incident waves, which can be regarded as flexible properties to control the wave radiation. Also, our model still works by breaking the space symmetry. Under this circumstance, the input wave with a much larger energy can be modulated by the control wave with less energy phenomenally. Our work enriches approaches on wave manipulation and may inspire related research studies on controllable absorption and radiation.

II. MODEL AND ANALYSIS

We take the acoustic system as an example to explain the underlying physics of the model. The conceptual diagram is shown in Fig. 1(a). The ZIM (green domain) with a circular dopant (yellow domain) embedded in it has been placed in the waveguide. The background medium is air with the constitution parameters of $\rho_a = 1.21$ kg/m^3 and $c_a = 343$ m/s. Here, ρ_a and c_a are the mass density and speed of sound, respectively. Accordingly, the effective parameters of the ZIM with matched impedance have been set as $\rho_Z = n\rho_a$ and $c_Z = c_a/n$ with an effective refractive index $n \to 0$, which can be realized by using several practical schemes described in previous works.[7,13,28–30] The mass density of the dopant is also assumed to approach zero, $\rho_D = \rho_Z$, while the speed of sound is taken as $c_D = c_a/n'$ with $n' = \sqrt{n(n + i\delta)}$. Here, δ is the variable to introduce the non-Hermitian modulation, which determines whether the dopant is a loss medium or a gain medium. Loss is inevitable in an acoustic measurement and can be well tuned as

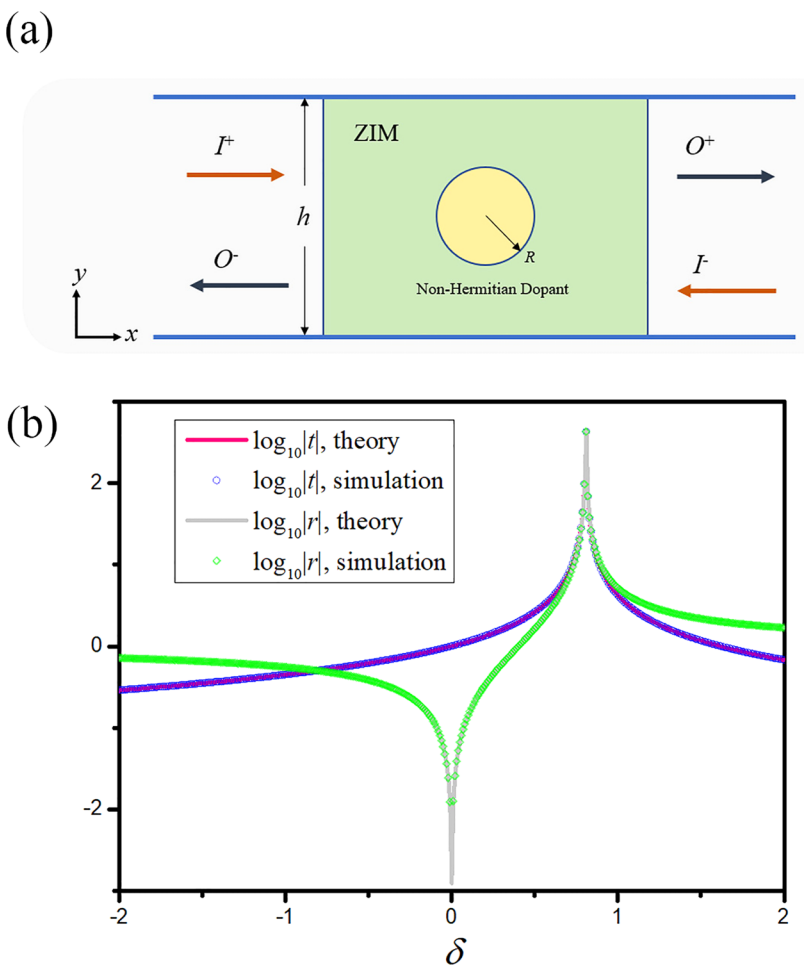

FIG. 1. (a) Schematic of the non-Hermitian dopant embedded in the ZIM. (b) Semilog plot of the transmission and reflection coefficients based on the theoretical derivation and numerical simulation.

required.[31,32] However, an acoustic gain medium can hardly be obtained naturally, but with the knowledge of active control[33] or electromechanical effects,[34] the acoustic gain effect can be experimentally observed through an elaborate design. Also, these active elements have their own dynamic ranges that can be adjusted for the input signals.

First, consider a plane wave $p_i = p_0 e^{-ik_0 x}$ incident from the left side, where p_0 and k_0 denote the amplitude and the wave number, respectively. We have omitted the time harmonic item $e^{i\omega t}$ for convenience. Note that the case with a two-side incidence can be treated as the linear superposition of a one-side incidence. Even though the ZIM has the matched impedance compared with the background medium, the existence of the dopant will generate the reflected wave p_r and transmitted wave p_t. Also, due to the property of the effective extremely large wavelength, the pressure field p_Z keeps a constant within the ZIM. Thus, combining the boundary condition of pressure, which is continuous at both sides of the ZIM, we can have the relationship $p_i + p_r = p_Z = p_t$, where $p_r = rp_i$ and $p_t = tp_i$. Here, r and t are employed to represent the reflection coefficient and transmission coefficient, respectively. Then, the following simplified expression can be obtained:

$$1 + r = t. \tag{1}$$

Moreover, as the pressure impinges on the circular dopant normally, the pressure field within the dopant can be expressed as $p_D = p_Z J_0(k'R')/J_0(k'R)$.[35] Here, $k' = n'k_0$ is the wave number of the dopant, R' is the relative radial coordinate, R is the radius, and J_0 denotes the zeroth order Bessel function. Since the ZIM is purely a passive medium without any gain or loss parts, applying the conservation of acoustic intensity flow to the domain of the ZIM, we can have $\oint pvdl = 0$, where l denotes the contour of the ZIM and $v = -\frac{1}{\rho}\int \nabla p dt$ is the particle velocity. Taking all boundaries of the ZIM into consideration, we can finally solve the transmission coefficient as follows:

$$t = \frac{1}{1 + \dfrac{i\pi R\rho_0 c_0 J_1(k'R)}{h\rho_D c_D J_0(k'R)}}. \tag{2}$$

For a quantitative description, we have set $R = 4$ mm, $h = 4R$, and the wavelength of the working frequency $\lambda = 2R$. We have also performed the simulations with commercial software COMSOL for the purposes of comparison. Both results have been presented in Fig. 1(b). It is clear that the results obtained from the theoretical derivation have good agreement with those derived from simulations with the same model. Particularly, in the Hermitian case with $\delta = 0$, the reflection coefficient reaches 0, while the transmission coefficient equals 1, indicating a total transmission guaranteed by the property of the ZIM.

We further investigate the case with two-side incidences. The red and black arrows, shown in Fig. 1(a), indicate the input (I) and output (O) acoustic waves. Since the model holds the mirror symmetry with reference to the middle plane of the sample, the transmission and reflection coefficients are the same for both propagation directions.[22] Then, the relation between the input waves and the output waves can be described by the matrix in the following form:

$$\begin{pmatrix} O^+ \\ O^- \end{pmatrix} = \begin{pmatrix} t & r \\ r & t \end{pmatrix} \begin{pmatrix} I^+ \\ I^- \end{pmatrix} = S \begin{pmatrix} I^+ \\ I^- \end{pmatrix}, \tag{3}$$

where the superscripts + and − denote the directions along and against the x axis, respectively. Obviously, the CPA mode and laser mode correspond to the zeros and poles of the scattering matrix S. By substituting Eqs. (1) and (2) into Eq. (3), the eigenvalues can be calculated analytically. We use $|s|$ to denote the intensity of the non-constant eigenvalue of S, which is also associated with the intensity of the outgoing waves.[21] The results have been plotted in Fig. (2).

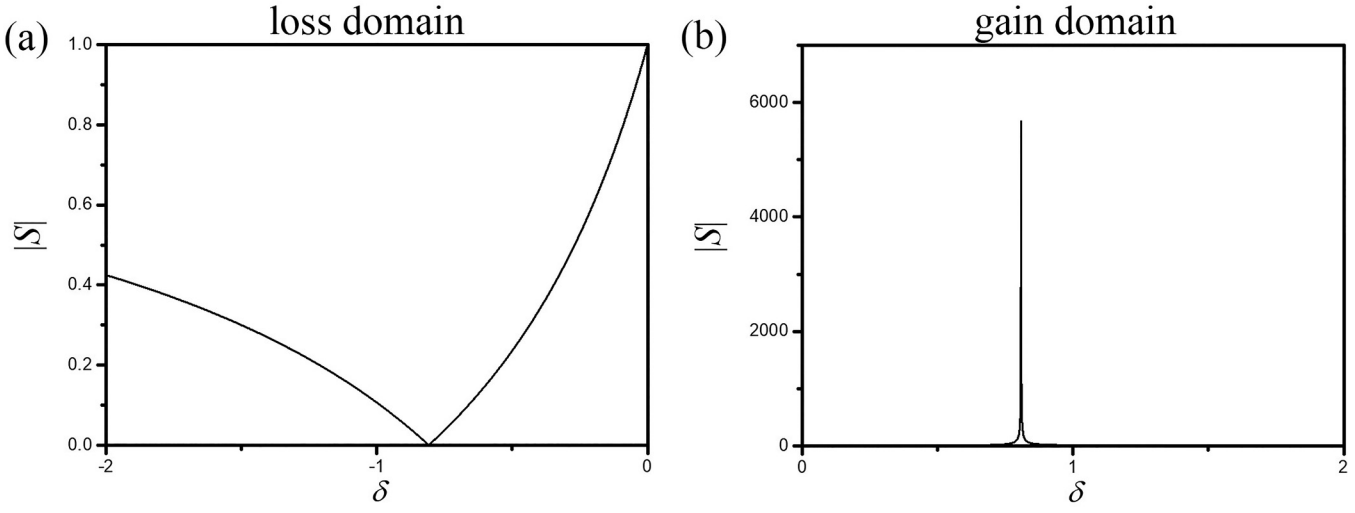

FIG. 2. The S-matrix eigenvalue intensity $|s|$ changes as a function of δ: (a) in the loss domain and (b) in the gain domain.

Figure 2(a) shows that in the loss domain with δ changing from -2 to 0, there indeed exists the zero point ($\delta = -0.808$) that indicates that the outgoing wave vanishes. Symmetrically, when the non-Hermitian modulation alters in the gain domain with δ changing from 0 to 2, the extreme point emerges at $\delta = 0.808$, as shown in Fig. 2(b). These two special points explicitly demonstrate how to generate the CPA mode and laser mode. Note that what we study here is the wave–matter interactions under ideal conditions. In the potential schemes for practical implementation, the system may need nonlinear parts, e.g., a limiter, for achieving a stable operation with restricted outgoing energy (cf. Appendix).

III. SIMULATIONS ON THE CPA AND LASER MODES

The full wave simulation based on the finite element method has been conducted to test the performance of the CPA and laser modes (see the supplementary material for a discussion on the simulations). Here, the length of the waveguide is $5a$ with $a = 1$ cm, and the length of the ZIM domain is $2a$. The ZIM domain is arranged in the middle of the waveguide and illuminated by the plane waves incident from both sides. To meet the critical requirement, the plane waves have the same amplitudes and initial phases. The pressure fields have been normalized to the incident waves in the following discussion. Figure 3(a) pictures the situation with $\delta = -0.808$, where the coherent perfect absorption arises. The white arrow represents the power flow in the field. Apparently, the acoustic energy flow from both sides impinges on the ZIM normally at first and is then redirected to the loss core. We also plot the pressure intensity along the x axis, as shown in Fig. 3(c). The distribution that holds the flat profile indicates that no reflected waves are generated at both sides of the ZIM and the incident waves have been absorbed perfectly. In the case of the laser mode at $\delta = 0.808$, as depicted in Fig. 3(b), the acoustic energy flow experiences the time-reversed process of the CPA mode and directs to both ports of the waveguide. Meanwhile, the amplitude of the pressure has received a great boost by the gain medium in the dopant, which can also be proved by the pressure intensity along the x axis in Fig. 3(d). The distribution also preserves the flat profile as the propagating wave but with a much larger amplitude than the incident waves. What needs to be emphasized here is that the position of the dopant embedded in the ZIM has no influence on the absorption/pumping performance due to the constant pressure field guaranteed by the properties of the ZIM.

IV. THE MODULATIONS ON THE PERFORMANCE

The flexible tunability of the CPA and laser modes plays an important role in potential applications. Figures 4(a) and 4(b) show the movement of the zeros and poles of $|s|$ in the parameter space of δ-R, respectively. In fact, the trajectories of zeros and poles follow the mirror symmetry with respect to the axis of $\delta = 0$. It also indicates that the dopant with a small size needs a larger

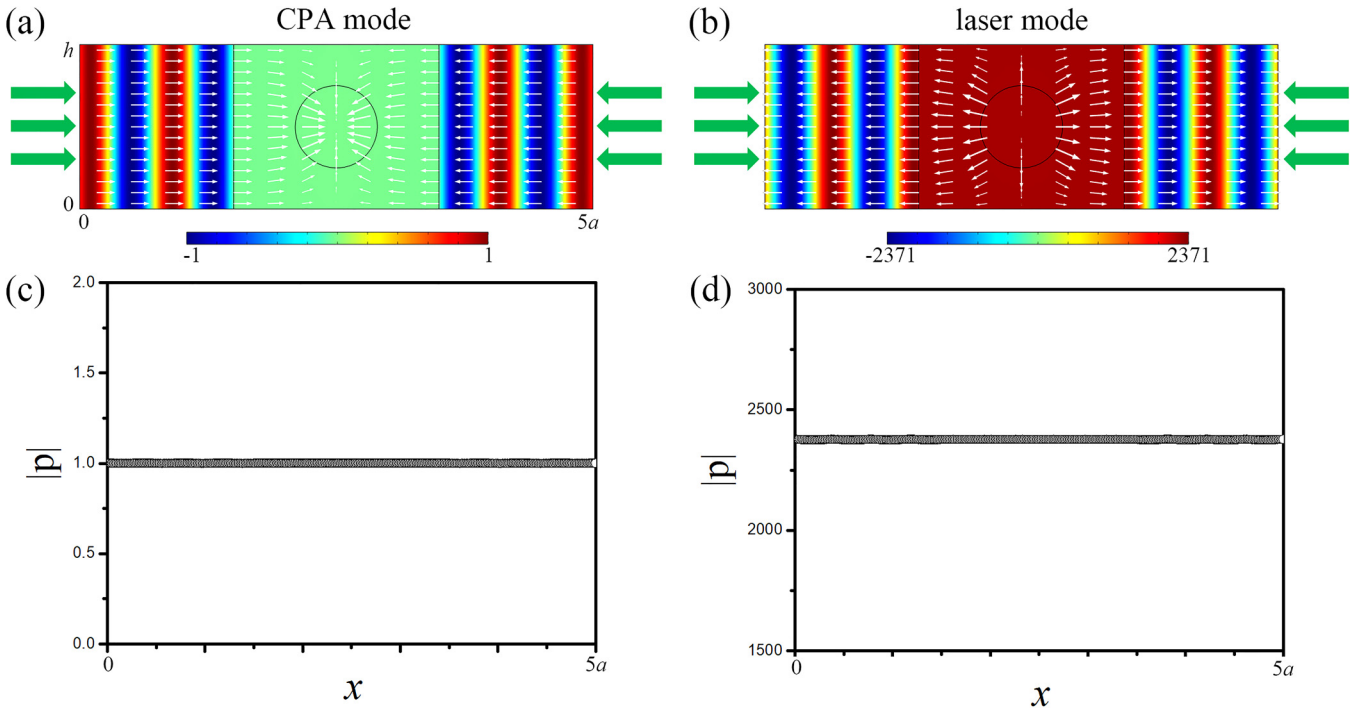

FIG. 3. The pressure field distribution for (a) the CPA mode and (b) the laser mode. The green arrows represent the incident waves with equal amplitude and phase. The white arrows represent the acoustic power flow. The corresponding intensities of pressure along the x axis for (c) the CPA mode and (d) the laser mode.

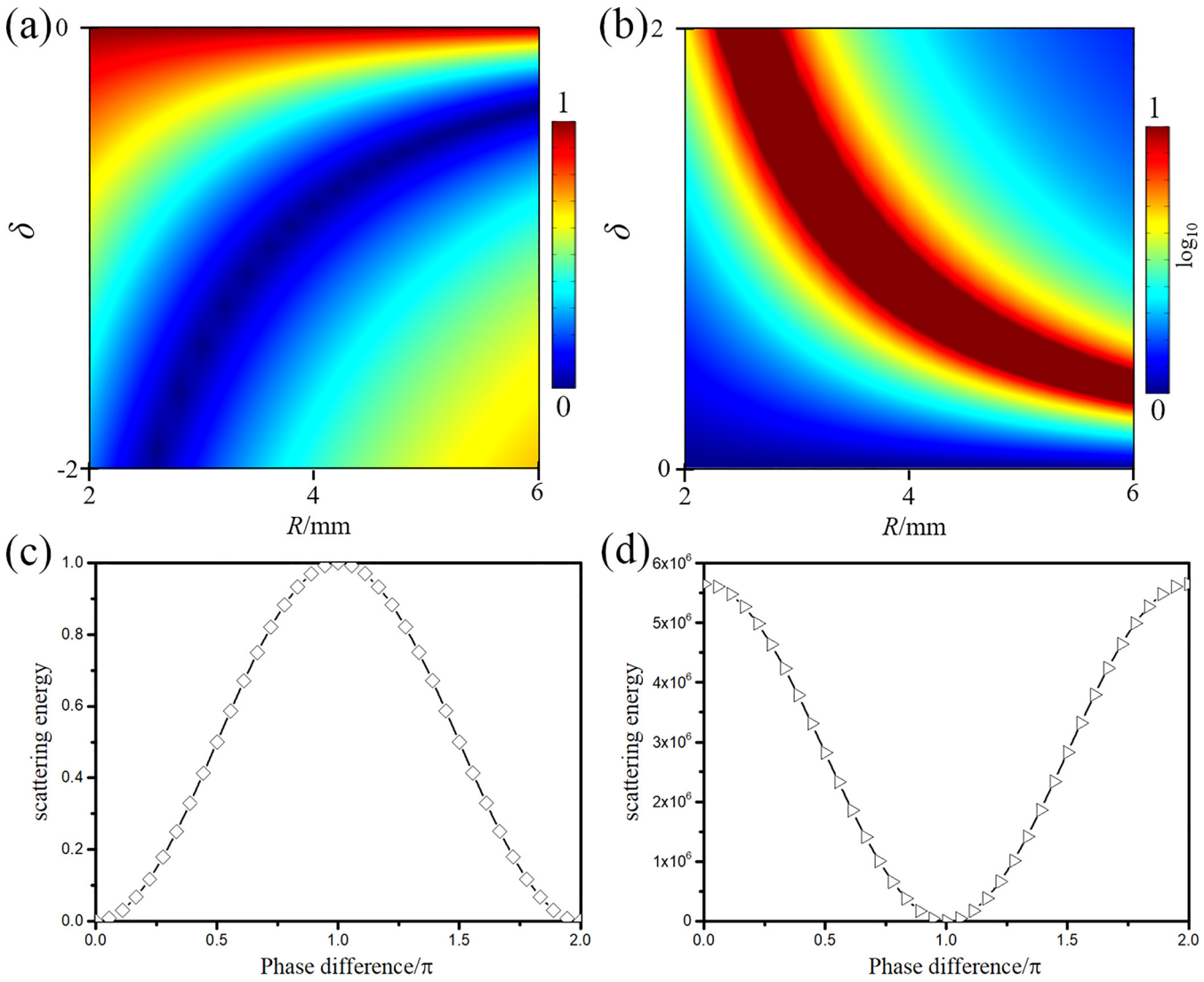

FIG. 4. The evolutions of the zeros (a) and poles (b) of $|s|$ in the parameter space of δ-R. The scattering energy as a function of phase difference for (c) the CPA mode and (d) the laser mode.

non-Hermitian modulation to create the CPA and laser modes, which is consistent with the physical intuitions. Moreover, as we have mentioned above, the performance of the CPA and laser can be easily controlled by changing the relative phase between the incident waves. We define the scattering energy as the output wave leaks from two ports $|O^+|^2 + |O^-|^2$ to evaluate this approach. The derived results as a function of the phase difference for the loss case and gain case have been plotted in Figs. 4(c) and 4(d), respectively. When the phase difference between the two incident waves is 0, we can undoubtedly achieve a perfect absorption performance and very high lasing efficiency. With adjusting the phase difference to π, the energy of the scattering waves increases in the CPA mode, while decreasing in the laser mode. When the phase difference equals π, the absorption and pumping effects are degenerated to total reflections due to the destructive interferences within the ZIM. After passing through it, the scattering energy for both cases is recovered to initial states since it is the relative phase that determines the performance.

Finally, we will discuss the case that asymmetric incident waves have different beam widths, as schematically shown in Fig. 5(a). The acoustic waves incident from both sides of the waveguide still have the same amplitude and initial phase, but the width of the right port of the waveguide has shrunk to $h/8$, which indicates that the acoustic energy emanating from the right side is

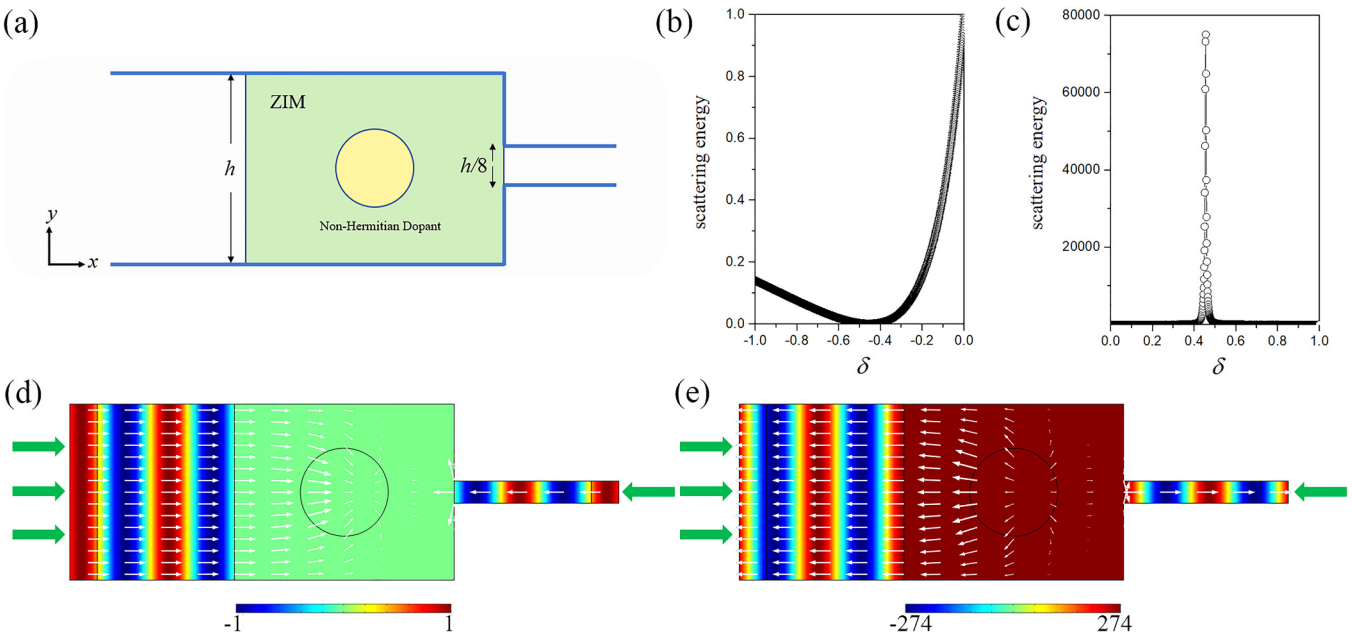

FIG. 5. (a) Schematic of the asymmetric incidence with different beam widths. The scattering energy vs the non-Hermitian modulation in (b) the loss domain and (c) gain domain. The pressure field distributions in (d) the CPA mode and (e) laser mode.

much less than that flowing from the left side. However, under this circumstance, the CPA and laser modes can still be stimulated with the non-Hermitian modulation. Figures 5(b) and 5(c) show the scattering energy as a function of δ in the loss domain and gain domain, respectively. The zero point of the scattering energy emerges at $\delta = -0.455$, where the coherent perfect absorption occurs. Also, the scattering energy equals 1 when $\delta = 0$, showing that the incident acoustic waves are scattered completely in the Hermitian case. In the gain domain, we can still find a pole point of the scattering energy at $\delta = 0.455$, where the outgoing waves are remarkably amplified. Here, the value of the intensity depends on the calculation accuracy, like the sweeping parameters, as no nonlinear part is considered in the simulations. The pressure fields for these two special modes have been calculated and plotted in Figs. 5(d) and 5(e). Similar to the symmetric structure, the incident acoustic waves from both sides are guided to the dopant and absorbed perfectly in the CPA mode. Conversely, in the laser mode, the incident waves are boosted and scattered at both sides evenly.

V. CONCLUSION

In conclusion, we propose and numerically demonstrate that the acoustic CPA mode and laser mode can be generated with the non-Hermitian dopant embedded in the ZIM. The sample can act as a perfect sink to absorb the acoustic waves in the CPA mode, while acting as a laser oscillator to amplify the incident waves in the laser mode. The performance of these intriguing scattering responses can be modulated by adjusting the size of the dopant or the relative phase between the incident waves. Counterintuitively, the input wave that carries a much larger energy can be tuned by the control wave that carries less energy to absorb or amplify the incident waves. Compared with the previous works with complex designs, our scheme provides a flexible approach to wave modulation with a non-Hermitian doped ZIM and may find potential applications in designing acoustic functional devices.

SUPPLEMENTARY MATERIAL

See the supplementary material for complete details on the finite element method simulation.

ACKNOWLEDGMENTS

This work was supported by the Research Grants Council of Hong Kong SAR (Grant Nos. C6013-18G, 15205219, and PolyU 152119/18E) and the National Natural Science Foundation of China (NNSFC) (Grant No. 11774297).

APPENDIX: SCHEME TO RESTRICT THE OUTPUT ENERGY

As we have mentioned above, in the potential schemes to realize the model practically, we often use active elements to construct a gain medium, e.g., the microphone and the loudspeaker. These active elements have their own dynamic ranges for the intensities of the input and output signals, which can be adjusted easily. Particularly, a limiter circuit that has an extremely large nonlinearity can be employed to make a system stable and protect the active

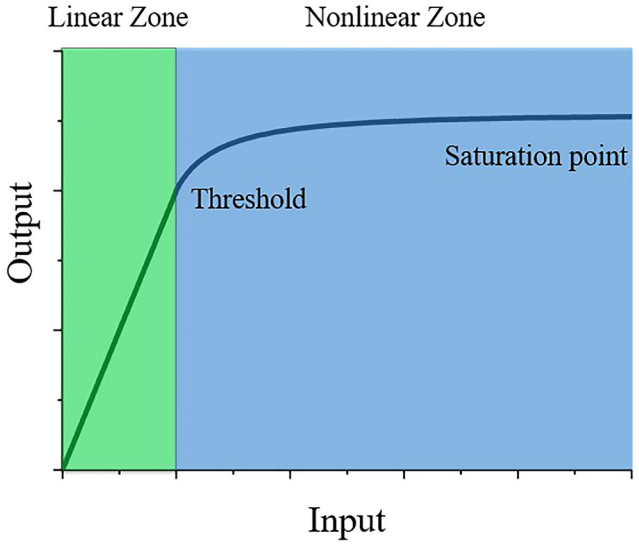

FIG. 6. The response relation between the input and the output signals.

elements from the overloaded energy. The response curve of a limiter is shown in Fig. 6. Below the threshold, the output signal will be rising linearly with increasing the input signal. However, beyond the threshold, the output signal will grow nonlinearly and reach a saturation value quickly. This strategy can effectively limit the intensity of the laser mode.

DATA AVAILABILITY

The data that support the findings of this study are available from the corresponding author upon reasonable request.

REFERENCES

[1]Y. Li, S. Kita, P. Muñoz, O. Reshef, D. I. Vulis, M. Yin, M. Lončar, and E. Mazur, "On-chip zero-index metamaterials," Nat. Photonics **9**, 738–742 (2015).
[2]P. Moitra, Y. Yang, Z. Anderson, I. I. Kravchenko, D. P. Briggs, and J. Valentine, "Realization of an all-dielectric zero-index optical metamaterial," Nat. Photonics **7**, 791–795 (2013).
[3]X. Huang, Y. Lai, Z. H. Hang, H. Zheng, and C. T. Chan, "Dirac cones induced by accidental degeneracy in photonic crystals and zero-refractive-index materials," Nat. Mater. **10**, 582–586 (2011).
[4]Y. Li, B. Liang, Z.-M. Gu, X.-Y. Zou, and J.-C. Cheng, "Unidirectional acoustic transmission through a prism with near-zero refractive index," Appl. Phys. Lett. **103**, 053505 (2013).
[5]Z.-M. Gu, B. Liang, X.-Y. Zou, J. Yang, Y. Li, J. Yang, and J.-C. Cheng, "One-way acoustic mirror based on anisotropic zero-index media," Appl. Phys. Lett. **107**, 213503 (2015).
[6]Y. Gu, Y. Cheng, J. Wang, and X. Liu, "Controlling sound transmission with density-near-zero acoustic membrane network," J. Appl. Phys. **118**, 024505 (2015).
[7]C. Xu, G. Ma, Z. G. Chen, J. Luo, J. Shi, Y. Lai, and Y. Wu, "Three-dimensional acoustic double-zero-index medium with a fourfold degenerate Dirac-like point," Phys. Rev. Lett. **124**, 074501 (2020).
[8]F. Liu and Z. Liu, "Elastic waves scattering without conversion in metamaterials with simultaneous zero indices for longitudinal and transverse waves," Phys. Rev. Lett. **115**, 175502 (2015).
[9]Z. Wang, W. Wei, N. Hu, R. Min, L. Pei, Y. Chen, F. Liu, and Z. Liu, "Manipulation of elastic waves by zero index metamaterials," J. Appl. Phys. **116**, 204501 (2014).
[10]R. Fleury and A. Alù, "Extraordinary sound transmission through density-near-zero ultranarrow channels," Phys. Rev. Lett. **111**, 055501 (2013).
[11]Y. Fu, L. Xu, Z. Hong Hang, and H. Chen, "Unidirectional transmission using array of zero-refractive-index metamaterials," Appl. Phys. Lett. **104**, 193509 (2014).
[12]C. Shen, Y. Xie, J. Li, S. A. Cummer, and Y. Jing, "Asymmetric acoustic transmission through near-zero-index and gradient-index metasurfaces," Appl. Phys. Lett. **108**, 223502 (2016).
[13]X.-F. Zhu, "Effective zero index in locally resonant acoustic material," Phys. Lett. A **377**, 1784–1787 (2013).
[14]I. Liberal, A. M. Mahmoud, Y. Li, B. Edwards, and N. Engheta, "Photonic doping of epsilon-near-zero media," Science **355**, 1058–1062 (2017).
[15]I. Liberal, Y. Li, and N. Engheta, "Reconfigurable epsilon-near-zero metasurfaces via photonic doping," Nanophotonics **7**, 1117–1127 (2018).
[16]M. Coppolaro, M. Moccia, G. Castaldi, N. Engheta, and V. Galdi, "Non-Hermitian doping of epsilon-near-zero media," Proc. Natl. Acad. Sci. U.S.A. **117**(25), 13921–13928 (2020).
[17]W. Wan, Y. Chong, L. Ge, H. Noh, A. D. Stone, and H. Cao, "Time-reversed lasing and interferometric control of absorption," Science **331**, 889–892 (2011).
[18]C. Meng, X. Zhang, S. T. Tang, M. Yang, and Z. Yang, "Acoustic coherent perfect absorbers as sensitive null detectors," Sci. Rep. **7**, 43574 (2017).
[19]Y. Sun, W. Tan, H. Q. Li, J. Li, and H. Chen, "Experimental demonstration of a coherent perfect absorber with PT phase transition," Phys. Rev. Lett. **112**, 143903 (2014).
[20]Y. D. Chong, L. Ge, and A. D. Stone, "PT-symmetry breaking and laser-absorber modes in optical scattering systems," Phys. Rev. Lett. **106**, 093902 (2011).
[21]Y. D. Chong, L. Ge, H. Cao, and A. D. Stone, "Coherent perfect absorbers: Time-reversed lasers," Phys. Rev. Lett. **105**, 053901 (2010).
[22]D. G. Baranov, A. Krasnok, T. Shegai, A. Alù, and Y. Chong, "Coherent perfect absorbers: Linear control of light with light," Nat. Rev. Mater. **2**, 17064 (2017).
[23]P. Wei, C. Croënne, S. Tak Chu, and J. Li, "Symmetrical and anti-symmetrical coherent perfect absorption for acoustic waves," Appl. Phys. Lett. **104**, 121902 (2014).
[24]J. Z. Song, P. Bai, Z. H. Hang, and Y. Lai, "Acoustic coherent perfect absorbers," New J. Phys. **16**, 033026 (2014).
[25]B. Baum, H. Alaeian, and J. Dionne, "A parity-time symmetric coherent plasmonic absorber-amplifier," J. Appl. Phys. **117**, 063106 (2015).
[26]J. Luo, B. Liu, Z. H. Hang, and Y. Lai, "Coherent perfect absorption via photonic doping of zero-index media," Laser Photonics Rev. **12**(8), 1800001 (2018).
[27]P. Bai, K. Ding, G. Wang, J. Luo, Z.-Q. Zhang, C. T. Chan, Y. Wu, and Y. Lai, "Simultaneous realization of a coherent perfect absorber and laser by zero-index media with both gain and loss," Phys. Rev. A **94**, 063841 (2016).
[28]M. Dubois, C. Shi, X. Zhu, Y. Wang, and X. Zhang, "Observation of acoustic Dirac-like cone and double zero refractive index," Nat. Commun. **8**, 14871 (2017).
[29]Z. Gu, H. Gao, T. Liu, Y. Li, and J. Zhu, "Dopant-modulated sound transmission with zero index acoustic metamaterials," J. Acoust. Soc. Am. **148**, 1636 (2020).
[30]M. Malléjac, A. Merkel, V. Tournat, J. P. Groby, and V. Romero-García, "Doping of a plate-type acoustic metamaterial," Phys. Rev. B **102**, 060302(R), (2020).
[31]H. Gao, H. Xue, Q. Wang, Z. Gu, T. Liu, J. Zhu, and B. Zhang, "Observation of topological edge states induced solely by non-hermiticity in an acoustic crystal," Phys. Rev. B **101**, 180303(R), (2020).
[32]T. Liu, G. Ma, S. Liang, H. Gao, Z. Gu, S. An, and J. Zhu, "Single-sided acoustic beam splitting based on parity-time symmetry," Phys. Rev. B **102**, 014306 (2020).
[33]C. Cho, X. Wen, N. Park, and J. Li, "Digitally virtualized atoms for acoustic metamaterials," Nat. Commun. **11**, 251 (2020).
[34]M. Willatzen, P. Gao, J. Christensen, and Z. L. Wang, "Acoustic gain in solids due to piezoelectricity, flexoelectricity, and electrostriction," Adv. Funct. Mater. **30**, 2003503 (2020).
[35]V. C. Nguyen, L. Chen, and K. Halterman, "Total transmission and total reflection by zero index metamaterials with defects," Phys. Rev. Lett. **105**, 233908 (2010).